International Journal of Mechanical Sciences 184 (2020) 105788

Contents lists available at ScienceDirect

International Journal of Mechanical Sciences

journal homepage: www.elsevier.com/locate/ijmecsci

Dynamic sensitivity-based finite element model updating for nonlinear structures using time-domain responses

Zhifu Cao[a], Qingguo Fei[a,*], Dong Jiang[a,b], Dahai Zhang[a], Hui Jin[c], Rui Zhu[a]

[a] Institute of Aerospace Machinery and Dynamics, Southeast University, Nanjing 211189, China
[b] School of Mechanical and Electronic Engineering, Nanjing Forestry University, Nanjing 210037, China
[c] Department of Engineering Mechanics, Southeast University, Nanjing 211189, China

ARTICLE INFO

Keywords:
Nonlinear model updating
Nonlinear structure
Time-domain response
Dynamic sensitivity
Direct differentiation method

ABSTRACT

A dynamic sensitivity-based model updating approach by using the time-domain responses is proposed in this paper. The sensitivity analysis of time-domain response is derived by using the direct differentiation method. The objective function of the nonlinear model updating is constructed by minimizing the discrepancy between the measured and the calculated time-domain responses. The time-domain responses and the corresponding dynamic sensitivities are calculated synchronously. The repeated nonlinear dynamic analysis can be avoided to obtain dynamic sensitivity, which is independent of the perturbation step. Numerical examples of a Duffing-Van der Pol oscillator, a magnetometer boom, and a cantilever plate with multiple nonlinear supports are adopted to verify the method. Crucial issues about the measured noise and the selection of the targeted responses are also considered and discussed. The validation results show that the proposed method is effectively applied to model updating of nonlinear structure using time-domain response with good anti-noise performance, and the scheme for response points selection is reliable for guaranteeing the accuracy.

1. Introduction

The finite element (FE) method has been widely applied in engineering, and many methods have been developed to improve the accuracy of the FE model [1–3]. Model updating is considered as the feasible approach for obtaining an updated model that accurately reflects structural responses under the linear hypothesis [4–6]. However, nonlinearities are widespread exist and cannot be neglected in practical structures [7-9]. To obtain a more accurate mathematical model to predict the nonlinear dynamic responses, therefore, the structural dynamic model updating methods for nonlinear structures have attracted attention.

In the conventional linear model updating methods, modal frequencies and mode shapes are considered as the output residuals to update the FE model [10–12]. However, these output residuals are not appropriate for the nonlinear dynamic behavior, since the nonlinear characteristics of the structures are difficult to be reflected from these outputs. Ewins et al. [13–15] proposed a 'modal test+' procedure for model validation of nonlinear engineering structures; the residual in the updating process was constructed using the nonlinear frequency response function. Wang et al. [16] presented a model updating strategy for structures with local nonlinearity, and nonlinear model updating was carried out after the underlying linear structure was updated. Similar to the 'modal test+' approach, the frequency domain responses were considered as the compared outputs. Asgarieh et al. [17] and Wang et al. [18,19] proposed a nonlinear model updating method based on the instantaneous modal parameters of the decomposed time-domain responses. Recently, with the application of the nonlinear normal modes (NNM) to structural dynamics, the NNM based nonlinear structural model updating methods [20–23] were presented and applied to the ECL [23] and Round Robin [20,21] benchmark problems. Silva et al. [24] and Asgarieh et al. [25] compared the frequency-domain and time-domain updating methods for nonlinear model updating. These different residuals, such as frequency response, nonlinear force, and time-varying instantaneous parameters, were proven to be successfully used for nonlinear updating. The time-domain responses contained the full effects of the nonlinearity in the structures are considered to construct the output residuals, which are requested to be minimized in the nonlinear model updating process.

The time-domain responses can be computed using different methods [26–29]. The effects of the nonlinear structural parameters on the time-domain responses are evaluated using the sensitivity analysis methods. Depending on whether the sensitivity is used, the model updating methods can be classified into gradient and non-gradient based algorithms. Song et al. [23] applied the interior point optimization algorithm, which does not require the gradients of the objective function to the updating parameters. In recent years, the intelligence-like algorithms [25,30,31] were successfully demonstrated to the non-gradient

* Corresponding author.
E-mail address: qgfei@seu.edu.cn (Q. Fei).

https://doi.org/10.1016/j.ijmecsci.2020.105788
Received 23 December 2019; Received in revised form 24 April 2020; Accepted 19 May 2020
Available online 23 May 2020

based nonlinear model updating method. Chisari et al. [32] proposed a genetic algorithm-based identification method to a based-isolated concrete bridge using the past dynamic and static test measurements. However, due to the global search, the whole updating procedure was often time-consuming. The sensitivity-based model updating methods were effective to the FE model updating but most of these applications are on the linear structures [33–36]. Ebrahimian et al. [37] proposed a framework for damage identification using the batch Bayesian estimation based nonlinear finite element updating approaches. The nonlinear dynamic behavior of the assembled structures is affected by the connections, and the structural model should be accurately updated using an effective nonlinear FE model updating method. A small number of attempts have been conducted on the sensitivity-based nonlinear FE model updating method. Using the nonlinear time-domain responses, the updating method based on the dynamic sensitivity is investigated in this paper.

The dynamic sensitivity is calculated using three methods: the finite difference method, the adjoint variable method, and the direct differentiation method. The finite difference method is simple to implement by each parameter perturbation; however, it suffers from the inefficiency caused by re-analysis for each parameter [38]. In the adjoint variable method, independent adjoint terms are added to the sensitivity equations of the objective function, and the sensitivities are computed in a manner analogous to the method of Lagrange multipliers [39]. In this approach, the nonlinear dynamic analysis with initial conditions became a terminal-value problem where terminal conditions were prescribed for the adjoint equations. These equations must be integrated backward in time, and the response and adjoint sensitivity cannot be computed simultaneously [40,41]. Meanwhile, the dynamic response and corresponding sensitivity can be synchronously determined using the direct sensitivity analysis method. Conte et al. [42] and Gu et al. [43] proposed the response sensitivity analysis approach to structure with plasticity material under dynamic loading conditions. Scott and Azad [44] applied the direct differentiation method to a force-based element formulation with material and geometric nonlinearity to compute the response sensitivities.

The dynamic sensitivity-based model updating method for structures with nonlinearity using the time-domain responses is proposed. This paper is organized as follows: In Section 2, the detailed formulation and nonlinear updating procedure of the dynamic sensitivity-based method are presented. To validate the performance of the proposed method, a Duffing-Van der Pol oscillator, a magnetometer boom structure with nonlinear hinges, and a cantilever plate with multiple nonlinear supports are adopted in Section 3. The conclusions are summarized in Section 4.

2. Methodology

To update the nonlinear FE model, the time-domain responses are selected as the targeted residual in the dynamic sensitivity-based updating process in this paper. The finite difference method can be used for calculating the dynamic sensitivity by repeated nonlinear dynamic analysis for each parameter. The method is time-consuming for large models and perturbation step dependent. The sensitivities of dynamic responses are calculated directly and synchronously using the direct differentiation method in this paper. Two types of nonlinear equations of motion are considered in this paper to derive the formulation of the dynamic sensitivity analysis. Based on the dynamic sensitivity analysis, the proposed nonlinear FE model updating procedure is introduced.

2.1. Dynamic sensitivity analysis for nonlinear structure

2.1.1. Formulation for the first-order sensitivity equation

The equation of motion for a nonlinear structure can be represented as

$$\mathbf{M}\ddot{\mathbf{x}}(t,\boldsymbol{\theta})+\mathbf{C}\dot{\mathbf{x}}(t,\boldsymbol{\theta})+\mathbf{K}\mathbf{x}(t,\boldsymbol{\theta})+\mathbf{f}_{nl}(\mathbf{x}(t,\boldsymbol{\theta}),\dot{\mathbf{x}}(t,\boldsymbol{\theta}),\boldsymbol{\theta})=\mathbf{f}(t) \tag{1}$$

where $\mathbf{M}$, $\mathbf{C}$, $\mathbf{K}\in\mathbb{R}^{N\times N}$ are the mass, damping, and stiffness matrix, respectively. $\mathbf{f}(t)\in\mathbb{R}^{N\times 1}$ represents the external excitation load. $\mathbf{x}(t,\boldsymbol{\theta})$, $\dot{\mathbf{x}}(t,\boldsymbol{\theta})$, $\ddot{\mathbf{x}}(t,\boldsymbol{\theta})\in\mathbb{R}^{N\times 1}$ are the displacement, velocity, and acceleration vector, respectively. $\mathbf{f}_{nl}(\mathbf{x}(t,\boldsymbol{\theta}),\dot{\mathbf{x}}(t,\boldsymbol{\theta}),\boldsymbol{\theta})\in\mathbb{R}^{N\times 1}$ is the nonlinear restoring force, in which case the nonlinear behavior of the structure is affected by the updating parameters $\boldsymbol{\theta}$. The first-order nonlinear equation of motion can be rewritten from Eq. (1):

$$\begin{cases}\dot{\boldsymbol{\eta}}(t,\boldsymbol{\theta})=\mathbf{F}(\boldsymbol{\eta}(t,\boldsymbol{\theta}),\boldsymbol{\theta},t)\\ \boldsymbol{\eta}(0,\boldsymbol{\theta})=\boldsymbol{\eta}_0\end{cases} \tag{2}$$

where $\boldsymbol{\eta}(t,\boldsymbol{\theta})=[\mathbf{x}(t,\boldsymbol{\theta})^T\ \dot{\mathbf{x}}(t,\boldsymbol{\theta})^T]^T$ is the $2N$-dimensional state vector, $\boldsymbol{\eta}_0$ is the initial conditions, and

$$\mathbf{F}(\boldsymbol{\eta}(t,\boldsymbol{\theta}),\boldsymbol{\theta},t)=\begin{pmatrix}\dot{\mathbf{x}}(t,\boldsymbol{\theta})\\ -\mathbf{M}^{-1}\left(\mathbf{C}\dot{\mathbf{x}}(t,\boldsymbol{\theta})+\mathbf{K}\mathbf{x}(t,\boldsymbol{\theta})+\mathbf{f}_{nl}(\mathbf{x}(t,\boldsymbol{\theta}),\dot{\mathbf{x}}(t,\boldsymbol{\theta}),\boldsymbol{\theta})-\mathbf{f}(t)\right)\end{pmatrix} \tag{3}$$

$\mathbf{F}(\boldsymbol{\eta}(t,\boldsymbol{\theta}),\boldsymbol{\theta},t)$ is the vector field.i The dynamic response sensitivity is computed by differentiating the Eq. (2) directly with respect to the design parameters θ_i (i=1,2,…, N_p), and applying the chain rule:

$$\begin{aligned}\frac{\partial\dot{\boldsymbol{\eta}}}{\partial\theta_i}&=\frac{\partial}{\partial\theta_i}\mathbf{F}(\boldsymbol{\eta}(t,\boldsymbol{\theta}),\boldsymbol{\theta},t)\\&=\nabla_{\boldsymbol{\eta}}\mathbf{F}(\boldsymbol{\eta}(t,\boldsymbol{\theta}),\boldsymbol{\theta},t)\cdot\frac{\partial\boldsymbol{\eta}}{\partial\theta_i}+\frac{\partial\mathbf{F}(\boldsymbol{\eta}(t,\boldsymbol{\theta}),\boldsymbol{\theta},t)}{\partial\theta_i}\end{aligned} \tag{4}$$

Similarly, the sensitivity equation is a first-order differentiation equation:

$$\begin{cases}\dfrac{d}{dt}\left(\dfrac{\partial\boldsymbol{\eta}}{\partial\theta_i}\right)=\nabla_{\boldsymbol{\eta}}\mathbf{F}(\boldsymbol{\eta}(t,\boldsymbol{\theta}),\boldsymbol{\theta},t)\cdot\dfrac{\partial\boldsymbol{\eta}}{\partial\theta_i}+\dfrac{\partial\mathbf{F}(\boldsymbol{\eta}(t,\boldsymbol{\theta}),\boldsymbol{\theta},t)}{\partial\theta_i}\\ \left.\dfrac{\partial\boldsymbol{\eta}}{\partial\theta_i}\right|_{t=0}=\mathbf{0}\end{cases} \tag{5}$$

Usually, the sensitivities of the initial displacement and velocity are zero, science the initial conditionsare given first. Obviously, similar to the direct sensitivity analysis based upon the second-order nonlinear equation of motion, Eq. (2) can be solved in conjunction with Eq. (5). The solutions of the nonlinear dynamic responses and corresponding sensitivities can be determined using the Runge-Kutta method, which is integrated into the 'ode45' function of MATLAB.

2.1.2. Formulation for the second-order sensitivity equation

The dynamic sensitivity for the nonlinear structure is also calculated by differentiating Eq. (1) directly with respect to the design parameters θ_i (i=1,2,…, N_p), the equation of the dynamic sensitivity is given by

$$\begin{aligned}\mathbf{M}\frac{\partial\ddot{\mathbf{x}}(t,\boldsymbol{\theta})}{\partial\theta_i}+\mathbf{C}\frac{\partial\dot{\mathbf{x}}(t,\boldsymbol{\theta})}{\partial\theta_i}+\mathbf{K}\frac{\partial\mathbf{x}(t,\boldsymbol{\theta})}{\partial\theta_i}&=-\frac{d\mathbf{f}_{nl}(\mathbf{x}(t,\boldsymbol{\theta}),\dot{\mathbf{x}}(t,\boldsymbol{\theta}),\boldsymbol{\theta})}{d\theta_i}\\&=-\left(\frac{\partial\mathbf{f}_{nl}(\mathbf{x}(t,\boldsymbol{\theta}),\dot{\mathbf{x}}(t,\boldsymbol{\theta}),\boldsymbol{\theta})}{\partial\mathbf{x}}\frac{\partial\mathbf{x}(t,\boldsymbol{\theta})}{\partial\theta_i}\right.\\&\quad\left.+\frac{\partial\mathbf{f}_{nl}(\mathbf{x}(t,\boldsymbol{\theta}),\dot{\mathbf{x}}(t,\boldsymbol{\theta}),\boldsymbol{\theta})}{\partial\dot{\mathbf{x}}}\frac{\partial\dot{\mathbf{x}}(t,\boldsymbol{\theta})}{\partial\theta_i}+\frac{\partial\mathbf{f}_{nl}}{\partial\boldsymbol{\theta}}\right)\\&=-\left(\mathbf{J}_{\mathbf{x}}\frac{\partial\mathbf{x}(t,\boldsymbol{\theta})}{\partial\theta_i}+\mathbf{J}_{\dot{\mathbf{x}}}\frac{\partial\dot{\mathbf{x}}(t,\boldsymbol{\theta})}{\partial\theta_i}+\frac{\partial\mathbf{f}_{nl}}{\partial\boldsymbol{\theta}}\right)\end{aligned} \tag{6}$$

where the last term in the right-hand side of this expression represents an explicit dependence on variable θ_i, and the first two terms show the implicit dependence through dynamic responses $\mathbf{x}$ and $\dot{\mathbf{x}}$. The symbols $\mathbf{J}_{\mathbf{x}}$ and $\mathbf{J}_{\dot{\mathbf{x}}}$are the Jacobian matrix of the nonlinear restoring force $\mathbf{f}_{nl}(\mathbf{x}(t,\boldsymbol{\theta}),\dot{\mathbf{x}}(t,\boldsymbol{\theta}),\boldsymbol{\theta})$ with respect to the displacement and velocity coordinates:

$$\mathbf{J}_{\mathbf{x}}=\begin{bmatrix}\frac{\partial f_{nl_1}}{\partial x_1}&\cdots&\frac{\partial f_{nl_1}}{\partial x_N}\\ \vdots&\ddots&\vdots\\ \frac{\partial f_{nl_N}}{\partial x_1}&\cdots&\frac{\partial f_{nl_N}}{\partial x_N}\end{bmatrix}\mathbf{J}_{\dot{\mathbf{x}}}=\begin{bmatrix}\frac{\partial f_{nl_1}}{\partial \dot{x}_1}&\cdots&\frac{\partial f_{nl_1}}{\partial \dot{x}_N}\\ \vdots&\ddots&\vdots\\ \frac{\partial f_{nl_N}}{\partial \dot{x}_1}&\cdots&\frac{\partial f_{nl_N}}{\partial \dot{x}_N}\end{bmatrix} \tag{8}$$

Introduce the following symbolic representation:

$$\begin{aligned}\mathbf{s}_i &= \frac{\partial \mathbf{x}(t,\boldsymbol{\theta})}{\partial \theta_i}\\ \dot{\mathbf{s}}_i &= \frac{\partial \dot{\mathbf{x}}(t,\boldsymbol{\theta})}{\partial \theta_i}\\ \ddot{\mathbf{s}}_i &= \frac{\partial \ddot{\mathbf{x}}(t,\boldsymbol{\theta})}{\partial \theta_i}\end{aligned} \tag{9}$$

the compact formula of the second-order ordinary differential equation of sensitivity can be rewritten as

$$\mathbf{M}\ddot{\mathbf{s}}_i + \left(\mathbf{C}+\mathbf{J}_{\dot{\mathbf{x}}}\right)\dot{\mathbf{s}}_i + \left(\mathbf{K}+\mathbf{J}_{\mathbf{x}}\right)\mathbf{s}_i + \frac{\partial \mathbf{f}_{nl}}{\partial \theta_i} = \mathbf{0} \tag{10}$$

With $\mathbf{x}(t,\boldsymbol{\theta})$ and $\dot{\mathbf{x}}(t,\boldsymbol{\theta})$ obtained from Eq. (1), the solution of the dynamic sensitivities can be computed from Eq. (10) using the Newmark-β method. The equilibrium equation of the nonlinear dynamic response sensitivity at t_{n+1} then can be derived as

$$\begin{aligned}\boldsymbol{\Phi}_{n+1} = {} & \mathbf{M}\left(-\frac{1}{\beta(\Delta t)^2}\mathbf{s}_{i,n} - \frac{1}{\beta(\Delta t)}\dot{\mathbf{s}}_{i,n} + \left(1-\frac{1}{2\beta}\right)\ddot{\mathbf{s}}_{i,n}\right)\\ & + \left(\mathbf{C}+\mathbf{J}_{\dot{\mathbf{x}},n+1}\right)\left(-\frac{\alpha}{\beta(\Delta t)}\mathbf{s}_{i,n} + \left(1-\frac{\alpha}{\beta}\right)\dot{\mathbf{s}}_{i,n} + (\Delta t)\left(1-\frac{\alpha}{2\beta}\right)\ddot{\mathbf{s}}_{i,n}\right)\\ & + \frac{\partial \mathbf{f}_{nl}\left(\mathbf{x}\left(t_{n+1},\boldsymbol{\theta}\right),\dot{\mathbf{x}}\left(t_{n+1},\boldsymbol{\theta}\right),\boldsymbol{\theta}\right)}{\partial \theta_i}\\ & + \left(\frac{1}{\beta(\Delta t)^2}\mathbf{M} + \frac{\alpha}{\beta(\Delta t)}\left(\mathbf{C}+\mathbf{J}_{\dot{\mathbf{x}},n+1}\right) + \left(\mathbf{K}+\mathbf{J}_{\mathbf{x},n+1}\right)\right)\mathbf{s}_{i,n+1}\\ = {} & \mathbf{0}\end{aligned} \tag{11}$$

in which Δt is the time-step. $\alpha(\alpha\geq 1/2)$ and $\beta(\beta\geq 1/4(\alpha+1/2)^2)$ are the integration constants, which guarantee the unconditional stability of the Newmark-β method [29]. The accuracy of the dynamic response solutions and the corresponding dynamic sensitivities depends on the time step [45], and the accuracy is guaranteed when using a sufficiently small time-step in this work.

The third term on the right-hand-side of Eq. (11) represents the partial derivative of the restoring force vector, $\mathbf{f}_{nl}(\mathbf{x}(t,\boldsymbol{\theta}),\dot{\mathbf{x}}(t,\boldsymbol{\theta}),\boldsymbol{\theta})$, with respect to interest parameter θ_i under the condition that the responses at time t_{n+1} are determined. The Jacobian matrix $\mathbf{J}_{\mathbf{x},n+1}$, and $\mathbf{J}_{\dot{\mathbf{x}},n+1}$ also should be determined using the responses at time t_{n+1}. This equation can be solved for the vector of unknowns $\mathbf{s}_{i,n+1}$. It should be noted that once the numerical response of the structure at t_{n+1} is known, the equilibrium equation of the nonlinear dynamic response sensitivity has several same structural matrices as Eq. (1) and is linear. Usually, the initial conditions of the displacement and velocity are given previously, which leads to the sensitivities of the initial conditions are zero. When the nonlinear dynamic response is also determined from the Newmark method, it is applied to compute the dynamic sensitivities directly at the current time. The advantage of the dynamic sensitivity analysis approach is that the response sensitivities can be synchronously computed with the nonlinear dynamic responses, either the first or second-order sensitivity analysis equations are applied.

2.2. Nonlinear finite element model updating procedure

The time-domain responses are useful outputs to update the nonlinear FE model. Without loss of generality, the calculated and measured dynamic response for the nonlinear structure are represented as $\mathbf{R}(t,\boldsymbol{\theta})$ and $\mathbf{R}^m$, respectively. As the first step in nonlinear FE model updating, the compared quantities can be collected in a vector such as

$$\mathbf{z}(t,\boldsymbol{\theta}) = \left[\mathbf{R}_1(t,\boldsymbol{\theta})^T,\cdots,\mathbf{R}_{Nq}(t,\boldsymbol{\theta})^T\right]^T \tag{12}$$

where N_q is the number of measured degrees-of-freedom (DOFs). The error is determined using the Taylor series expansion of the calculated outputs truncated after the linear term:

$$\boldsymbol{\varepsilon}_z = \mathbf{z}^m - \mathbf{z}(t,\boldsymbol{\theta}) \approx \mathbf{r}_j - \mathbf{S}_j\left(\boldsymbol{\theta}-\boldsymbol{\theta}_j\right) \tag{13}$$

in which the vector, $\mathbf{r}_j=\mathbf{z}^m-\mathbf{z}_j$, is defined as the difference between the measured and calculated outputs at the jth iteration. The measured and calculated outputs are denoted by $\mathbf{z}^m$ and $\mathbf{z}_j=\mathbf{z}(\boldsymbol{\theta}_j)$. $\mathbf{S}_j$ is the sensitivity matrix in the jth iteration. The error, $\boldsymbol{\varepsilon}_z$, is assumed to be small for parameters $\boldsymbol{\theta}$ in the vicinity of $\boldsymbol{\theta}_j$, and at each iteration, the Eq. (13) is solved for

$$\Delta\boldsymbol{\theta}_j = \boldsymbol{\theta}-\boldsymbol{\theta}_j \tag{14}$$

The updated parameters are then given by

$$\boldsymbol{\theta}_{j+1} = \boldsymbol{\theta}_j + \Delta\boldsymbol{\theta}_j \tag{15}$$

In practice, the model updating is carried out by minimizing the error:

$$\min_{\boldsymbol{\theta}\in(\mathbb{R})^{p\times 1}:\boldsymbol{\theta}_l\leq\boldsymbol{\theta}\leq\boldsymbol{\theta}_u} \frac{1}{2}\boldsymbol{\varepsilon}_z(\boldsymbol{\theta})^T\mathbf{W}\boldsymbol{\varepsilon}_z(\boldsymbol{\theta}) \tag{16}$$

where $\mathbf{W}$ is the diagonal weighting matrix that accounts for the importance of each individual term in the error vector. $[\boldsymbol{\theta}_l,\boldsymbol{\theta}_u]$ is the parameter interval for the varying of the updating parameters. The objective function is then rewritten as the following weighted square Euclidean norm of the error vector:

$$\begin{aligned}J_{non}(\boldsymbol{\theta}) &= \frac{1}{2}\sum_{q=1}^{N_q}\sum_{k=1}^{N_t} \| W_{\mathbf{z}(t,\boldsymbol{\theta})}\left(R_q^m\left(t_k\right) - R_q\left(t_k,\boldsymbol{\theta}\right)\right)\|_2^2\\ &:= \frac{1}{2}\| \mathbf{W}_{\mathbf{z}(t,\boldsymbol{\theta})}(\mathbf{z}^m(t)-\mathbf{z}(t,\boldsymbol{\theta}))\|_2^2\end{aligned} \tag{17}$$

in which $\mathbf{W}_{\mathbf{z}(t,\boldsymbol{\theta})}$ can be obtained by $\mathbf{W}_{\mathbf{z}(t,\boldsymbol{\theta})}$, $||\bullet||$ means the L_2-norm. In general, the weighting matrix is difficult to be estimated; some reasonable choices are given by a previous study [4]. In this paper, the weighting matrix for nonlinear FE model updating is $\mathbf{W}=\mathbf{I}$, which denotes no scales for the time-domain responses.

Since the relationship between the outputs vector $\mathbf{z}(t,\boldsymbol{\theta})$ and the updating parameters $\boldsymbol{\theta}$ is nonlinear, the minimization of Eq. (17) leads to a nonlinear least square problem, which is solved by iterative methods. In the model updating problem, the derivatives $\partial J_{non}/\partial\Delta\boldsymbol{\theta}=\mathbf{0}$ are required to the minimization of the objective equation Eq. (17), which yields after substitution of Eq. (13) the following equation at jth iteration,

$$\mathbf{W}_{\mathbf{z}(t,\boldsymbol{\theta})}\mathbf{S}_j\Delta\boldsymbol{\theta}_j = \mathbf{W}_{\mathbf{z}(t,\boldsymbol{\theta})}\mathbf{r}_j \tag{18}$$

In parameter updating by using the time-domain responses, the number of measurements is always made larger than the number of parameters that yields overdetermined equation systems. Thus, the parameter changes can be solved from the following equation:

$$\mathbf{S}_j^T\mathbf{W}_{\mathbf{z}(t,\boldsymbol{\theta})}\mathbf{S}_j\Delta\boldsymbol{\theta}_j = \mathbf{S}_j^T\mathbf{W}_{\mathbf{z}(t,\boldsymbol{\theta})}\mathbf{r}_j \tag{19}$$

The solution $\Delta\boldsymbol{\theta}_j$ can be determined using the optimization method in MATLAB. The sensitivity matrix of dynamic responses with respect to updating parameters at jth iteration is given as

$$\mathbf{S}_j = \left[\frac{\partial \mathbf{z}_j}{\partial \boldsymbol{\theta}}\right]_{\boldsymbol{\theta}=\boldsymbol{\theta}_j} = \begin{bmatrix} \frac{\partial R_1(t_1)}{\partial \theta_1} & \frac{\partial R_1(t_1)}{\partial \theta_2} & \cdots & \frac{\partial R_1(t_1)}{\partial \theta_{N_p}} \\ \vdots & \vdots & \ddots & \vdots \\ \frac{\partial R_1(t_{N_t})}{\partial \theta_1} & \frac{\partial R_1(t_{N_t})}{\partial \theta_2} & \cdots & \frac{\partial R_1(t_{N_t})}{\partial \theta_{N_p}} \\ \hdashline \frac{\partial R_2(t_1)}{\partial \theta_1} & \frac{\partial R_2(t_1)}{\partial \theta_2} & \cdots & \frac{\partial R_2(t_1)}{\partial \theta_{N_p}} \\ \vdots & \vdots & \ddots & \vdots \\ \frac{\partial R_2(t_{N_t})}{\partial \theta_1} & \frac{\partial R_2(t_{N_t})}{\partial \theta_2} & \cdots & \frac{\partial R_2(t_{N_t})}{\partial \theta_{N_p}} \\ \hdashline \vdots & \vdots & \ddots & \vdots \\ \hdashline \frac{\partial R_{N_q}(t_1)}{\partial \theta_1} & \frac{\partial R_{N_q}(t_1)}{\partial \theta_2} & \cdots & \frac{\partial R_{N_q}(t_1)}{\partial \theta_{N_p}} \\ \vdots & \vdots & \ddots & \vdots \\ \frac{\partial R_{N_q}(t_{N_t})}{\partial \theta_1} & \frac{\partial R_{N_q}(t_{N_t})}{\partial \theta_2} & \cdots & \frac{\partial R_{N_q}(t_{N_t})}{\partial \theta_{N_p}} \end{bmatrix}_{N_q \cdot N_t \times N_p} \tag{20}$$

where $\mathbf{S}_j$ is determined using the dynamic sensitivity analysis method that is introduced in Section 2.1.

The dynamic sensitivity-based nonlinear FE model updating method is illustrated in Fig. 1. The process starts with the initial FE modeling considering some nonlinear features, and the measured responses. By using the calculated and measured responses, the response residual that describes the analysis/real discrepancies is constructed. The dynamic sensitivity analysis procedure is conducted to compute the dynamic responses and corresponding derivatives with respect to updating parameters synchronously. The process continues with parameter estimation to produce an incremental parameter for an updated nonlinear FE model. Afterward, the implementation steps of the method are explained in detail and the pseudo-codes for dynamic sensitivity analysis and nonlinear FE model updating are illustrated in Appendix A.

Step 1: Construct the FE model of the nonlinear structure. The commercial FE software, e.g., NASTRAN, is used for exporting the structural matrices of the linear component that ensures the proposed method to be applicable for complex structure. The nonlinear force is added to the FE model using MATLAB, in which the nonlinear dynamic analysis and updating are carried out.

Step 2: Determine whether the measured responses match well with the calculated responses of the nonlinear model. If not, begin the sensitivity-based nonlinear model updating procedure.

Step 3: Select the targeted response points and construct the residuals between the measured and calculated responses.

Step 4: Select the updating parameters and conduct the nonlinear response sensitivity analysis using the proposed formulations of first- or second-order sensitivity equations using the direct differentiation method.

Step 5: Determine the parameter changes $\Delta\theta_j$ using the direct sensitivity-based optimization algorithm and estimate whether the response errors or parameter estimation errors satisfy the convergence criterion. If not, continue the procedure by re-analysis of the nonlinear structure using the new parameters.

Step 6: Stop the nonlinear model updating procedure until any of the response errors or parameter estimation errors satisfy the convergence criterion. If not, repeat Steps 3 to 6 until the number of iterations equals to the maximum number. The response error e_r (e.g. 10^{-6}) and parameter estimation error e_θ (e.g. 10^{-6}) are defined as

$$e_r = \frac{\|\mathbf{R}^m - \mathbf{R}\|_2}{\|\mathbf{R}^m\|_2} \times 100\% \tag{21}$$

$$e_\theta = \frac{\|\Delta\boldsymbol{\theta}\|_2}{\|\boldsymbol{\theta}\|_2} \times 100\% \tag{22}$$

The dynamic sensitivity analysis plays an important role in the proposed nonlinear FE model updating procedure. The proposed method is challenging to update the structures with non-smooth nonlinearity, as the sensitivity of the dynamic responses with respect to non-smooth parameters is hard to be computed using the direct sensitivity analysis method. Two crucial issues are considered in the proposed nonlinear model updating procedure. The first is that the measured time-domain responses generally have some random noise. This negatively affects the accuracy of the parameter updating. In this study, the polluted measurements are simulated with zero-mean Gaussian white noise [46] added to the calculated acceleration as

$$\hat{\mathbf{R}}^m = \mathbf{R} + N_l \cdot \mathbf{N}_{oise} \cdot var(\mathbf{R}) \tag{23}$$

where $\hat{\mathbf{R}}^m$ is the vector of polluted acceleration; N_l is the noise level; $\mathbf{N}_{oise}$ is a standard normal distribution vector with zero mean and unit standard deviation; $var(*)$ means the variance of the time history; $\mathbf{R}$ is the vector of calculated acceleration. The other is the selection of the targeted responses used in nonlinear FE model updating. As is well known, chaotic behavior is exhibited in some nonlinear systems for specific values of parameters. When applying the time-domain responses as the targeted outputs, the long-term behavior of nonlinear systems is often sensitive to the change of parameters, but short-term behavior is not [47]. The selection of time points should be controlled by introducing a selection control variable, e.g. γ, into the objective function.

$$J_{non}(\boldsymbol{\theta}) = \frac{1}{2}\sum_{q=1}^{N_q}\sum_{k=1}^{\gamma N_t} \| W_{\mathbf{z}(t,\boldsymbol{\theta})}\left(R_q(t_k,\boldsymbol{\theta}) - R_q^m(t_k)\right)\|_2^2, with\ \gamma \in (\gamma_{\min}, 1] \tag{24}$$

in which the minimal $\gamma_{\min} > N_q/N_t$ ensures the existence of the optimal solution.

3. Case studies

The performance of the proposed direct sensitivity-based approach is demonstrated by updating three nonlinear models: Duffing-Van der Pol oscillator, a magnetometer boom, and a cantilever plate with multiple nonlinear supports. For computational cases, the forced external excitation or free vibration are simulated to three examples with given initial conditions. For all case studies, the formulation and location of the nonlinearity are assumed to be known beforehand, and the critical issues are focused on the verification and implementation of the proposed method. Discussions on the measurement noise and selection of the targeted responses are also conducted to the proposed method.

3.1. Duffing-Van der Pol oscillator

Duffing-Van der Pol oscillator, a non-autonomous system, is the most extensively studied example of nonlinear systems because of its wide

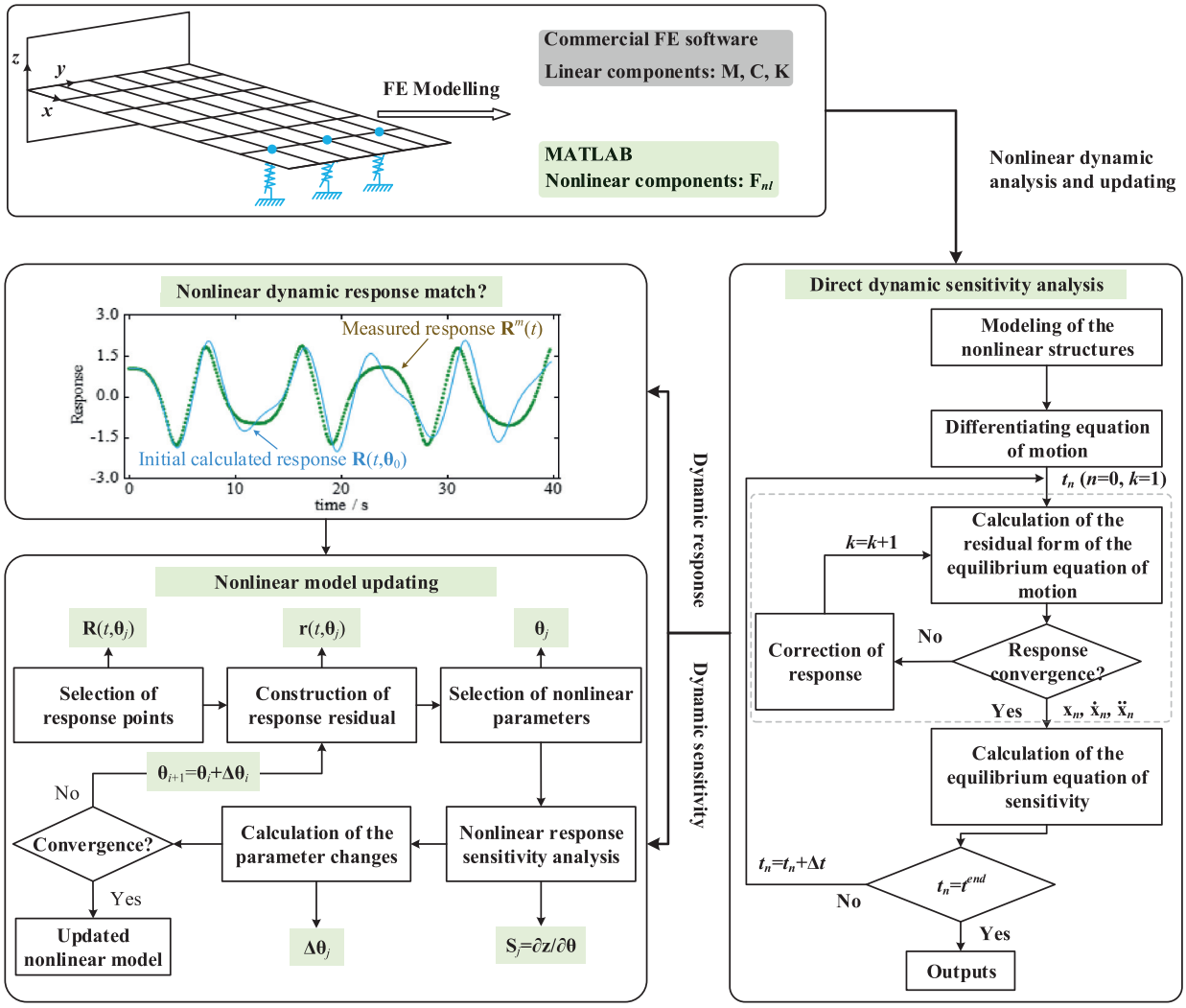

Fig. 1. Flow chart for the direct sensitivity-based model updating using the time-domain responses combined with MATLAB and commercial FE software.

range of dynamic behaviors. Examples of such behavior arise in several mechanical engineering applications [48,49]. The non-dimensional motion of the oscillator subject to harmonic external excitation load is the following

$$\ddot{x}(t) - \mu\left(1 - x^2(t)\right)\dot{x}(t) + \alpha x(t) + \beta x^3(t) = f\cos(\omega t) \tag{25}$$

in which $x(t)$ is the displacement of the oscillator, $\mu(\mu>0)$ is the damping parameter, α and β are the system parameters, $f(f=1)$ and $\omega(\omega=0.79)$ is the amplitude and frequency of the harmonic external excitation load. Herein, the dynamic response sensitivity is calculated upon the first-order form of the oscillator

$$\begin{cases} \dot{x} = y \\ \dot{y} = \mu\left(1 - x^2(t)\right)\dot{x}(t) - \alpha x(t) - \beta x^3(t) + f\cos(\omega t) \end{cases} \tag{26}$$

The detailed formulations of the dynamic response and sensitivity analysis are given in Appendix B. Initial conditions are $x(0)=1$ and $y(0)=0$. The time interval is [0, 50]s, and the corresponding time step is $\Delta t=0.01$, which guarantees the accuracy for computing the nonlinear dynamic responses and sensitivities. The simulated dynamic responses and corresponding dynamic sensitivities are solved by the 'ode45' function of MATLAB. The oscillator takes three main physical behavior by adopting different values of system parameters, and the exact parameters are given as follows.

- Single well, if $\alpha>0$, $\beta>0$: $\mu=0.1$, $\alpha=0.5$, $\beta=0.5$;
- Double well, if $\alpha<0$, $\beta>0$: $\mu=0.1$, $\alpha=-0.5$, $\beta=0.5$;
- Double-hump, if $\alpha>0$, $\beta<0$: $\mu=0.5$, $\alpha=3$, $\beta=-0.2$.

Table 1
Initial parameters of the Duffing-Van der Pol oscillator for different measurement noise.

Parameters	μ	α	β
Case 1	0.04	0.8	0.2
Case 2	0.06	-0.7	0.3
Case 3	0.4	3.6	-0.16

The following three initial cases, which are listed in Table 1, are used for nonlinear model updating considering measurement noise. Measurement noise with different levels N_l=0, 0.5%, 1%, 2%, 5% is enforced to investigate the robustness of the proposed approach. The displacements of three cases are considered as the targeted outputs, and the default control variable for the selection of the targeted responses are γ=0.2, 0.2, and 0.06 for case 1, 2, and 3, respectively. The phase diagrams of the measured responses with high noise level (N_l=5%) are shown in Fig. 2.

By adopting the proposed dynamic sensitivity-based model updating method, the relative ratio for the updated parameters is presented in

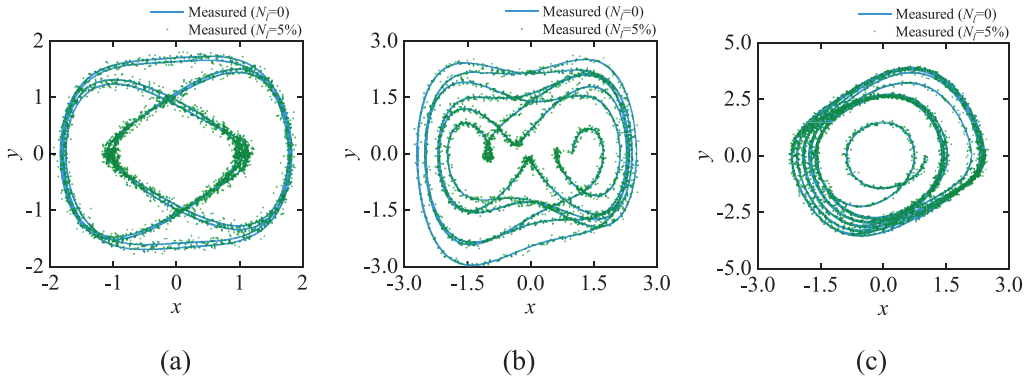

Fig. 2. Phase diagrams of the measured responses with different noise level for three cases: (a) Case 1: μ=0.04, α=0.8, β=0.2, N_l=0 and 5%; (b) Case 2: μ=0.06, α=-0.7, β=0.3, N_l=0 and 5%; (c) Case 3: μ=0.4, α=3.6, β=-0.16, N_l=0 and 5%.

Table 2
The relative ratio for the updated parameters for Duffing-Van der Pol oscillator with different measurement noise levels.

Noise level		N_l=0	N_l=0.5%	N_l=1%	N_l=2%	N_l=5%
Case 1	r_μ	1.000	1.003	0.984	0.945	0.925
	r_α	1.000	0.999	0.999	0.989	0.987
	r_β	1.000	1.000	1.001	1.010	1.014
Case 2	r_μ	1.000	1.001	1.000	0.997	0.999
	r_α	1.000	0.999	0.996	0.996	1.014
	r_β	1.000	1.000	0.999	0.999	1.001
Case 3	r_μ	1.000	1.000	1.000	1.007	1.019
	r_α	1.000	1.000	1.000	1.000	0.999
	r_β	1.000	0.992	0.997	1.016	0.969

Table 2 and defined as

$$r_i = \frac{\theta_i^{updated}}{\theta_i^{exact}}, \theta_i \in \boldsymbol{\theta} \tag{27}$$

where θ^{exact} represents the exact parameter, and r denotes the relative ratios retained three digits after the decimal point. The convergence criterion of the response error and parameter estimation error are e_r=10^{-6} and e_θ=10^{-6}, respectively. The updated parameters are close to the exact parameters when the relative ratio is close to 1. The relative error also can be calculated by using the relative ratio $e_{\theta i}$=$|r_i$-1$|$×100%. As shown in Table 2, in case of no noise, the parameters are successfully updated, nevertheless, the relative ratio of these cases reaches 0.992 ($e_{\max}$=0.8%) for noise level N_l=0.5% and equals to 0.984 ($e_{\max}$=1.6%) for N_l=1%, respectively. Results indicate that the parameters are well updated when the observation with low noise. The maximum error of the updated parameters increases with the increasing of the measurement noise. When the high measurement noise levels are considered, e.g., N_l=2% and N_l=5%, the relative ratios are 0.945 ($e_{\max}$=5.5%) and 0.925 ($e_{\max}$=7.5%), respectively. The proposed dynamic sensitivity-based nonlinear FE model updating method has limitation on the case that the observations with high measurement noise.

To investigate the effect of the selection of the targeted responses, the oscillator with measurement noise N_l=1% but on different control variable is considered. A small value of γ denotes a small amount of time-domain responses are selected as targeted responses. In this case, a small to large control variable is considered: γ=0.06, 0.2, 0.5, and 0.8, and the numbers of targeted responses are 300, 1000, 2500, and 4000, respectively.

The initial parameters are listed in Table 3 for the discussion on the selection of the targeted responses. The measured and different targeted response selections for three cases are shown in Fig. 3. The difference between the initial and targeted responses increases with the increase of the variable γ. After the nonlinear model updating process, the corresponding relative ratios are presented in Table 4 in detail. It is observed

Table 3
Initial parameters to the investigation on the selection of the targeted responses.

Parameters	μ	α	β
Case I	0.06	0.7	0.3
Case II	0.06	-0.7	0.3
Case III	0.3	4.2	-0.12

Table 4
The relative ratio of the updated parameters for Duffing-Van der Pol oscillator with different selection control variable γ.

r		γ=0.06	γ=0.2	γ=0.5	γ=0.8
Case I	r_μ	1.035	1.019	0.956	3.600
	r_α	0.997	1.001	0.998	1.631
	r_β	1.003	0.999	1.002	0.708
Case II	r_μ	1.066	1.000	1.001	0.999
	r_α	1.001	0.996	0.999	1.001
	r_β	1.001	0.999	1.000	1.000
Case III	r_μ	0.998	-	-2.400	-2.400
	r_α	1.004	-	0.774	1.854
	r_β	1.055	-	3.600	3.600

that the parameters of case II can be accurately updated for these four control variables based on the proposed method. The relative ratios for cases I and III are far away from 1 with an increasing of the variable γ, and the parameters become unable to be updated when γ increases to 0.8 (case I) and 0.2~0.8 (case III). This is explainable since the discrepancy of the targeted responses, as shown in Fig. 3, increases with the increase of γ. Results show that, when the relative error of the initial responses is significant, the accuracy of the updated parameters can be ensured when using a small γ>N_q/N_t.

3.2. Magnetometer boom

Considering a general nonlinear hinge in the space structure, the proposed method is implemented for updating the local parameters of the nonlinear hinge elements. As shown in Fig. 4, an example of a space structure magnetometer, which is used to measure the strength and the direction of the local magnetic field in satellites, such as LISA [50], SMILE [51]. The articulated magnetometer generally consists of booms, hinges, and sensors. The folded and deployed configuration of the magnetometer is shown in Fig. 4 (a) and (b), respectively.

As shown in Fig. 4(c), the three hinges are modeled using the nonlinear spring elements, and the booms are modeled using the simple beam elements. The geometrical and material parameters of the fluxgate magnetometer are listed in Table 5. It should be noted that

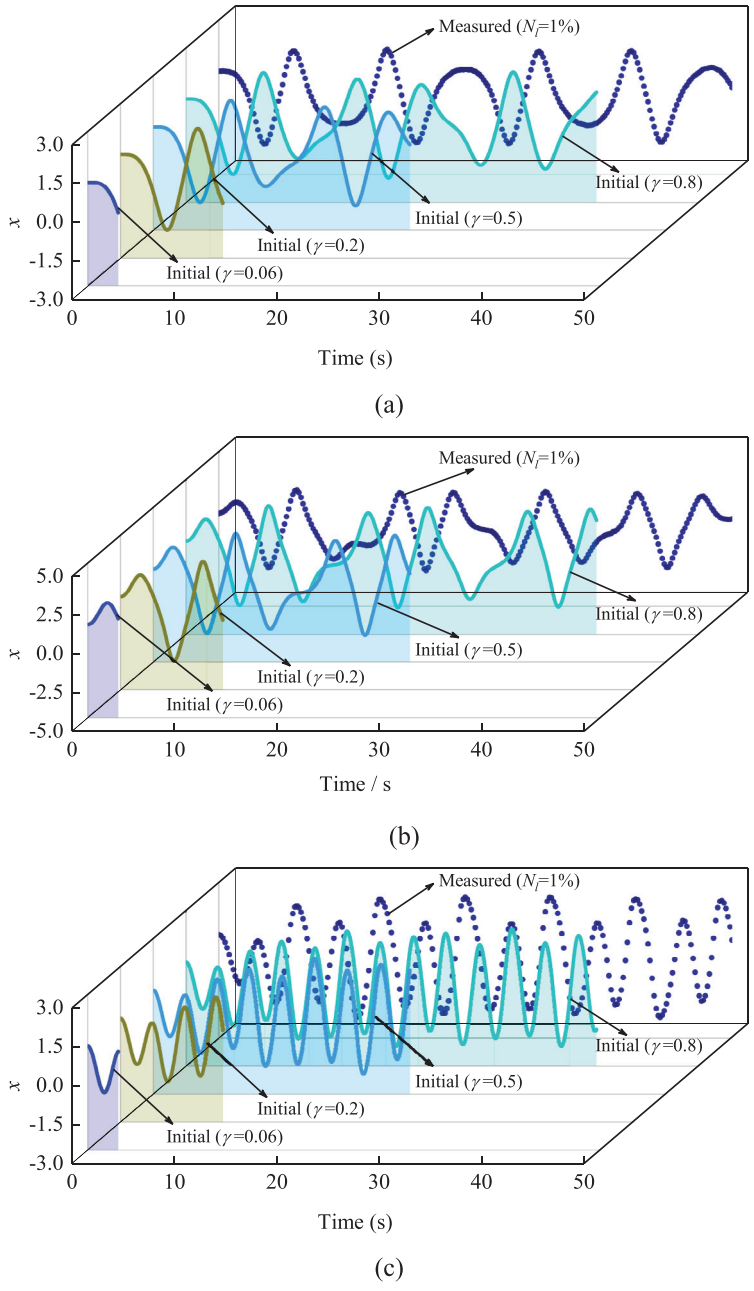

Fig. 3. Measured responses and the selected targeted responses with different control variables: (a) Case I: μ=0.06, α=0.7, β=0.3; (b) Case II: μ=0.06, α=-0.7, β=0.3; (c) Case III: μ=0.3, α=4.2, β=-0.12.

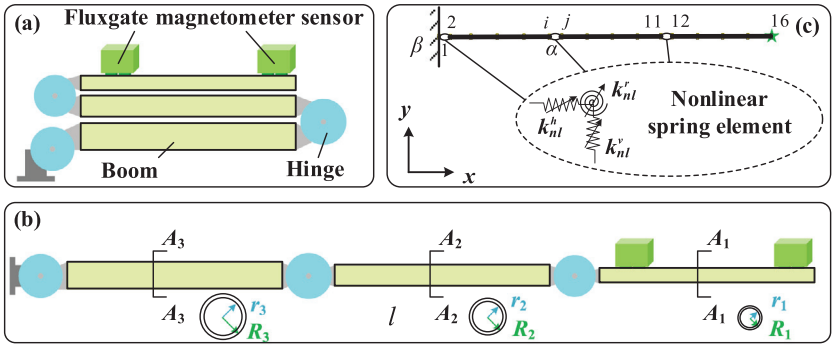

Fig. 4. An example of a fluxgate magnetometer in (a) folded and (b) deployed configuration, and (c) the finite element model with nonlinear spring elements.

Table 5
Parameters of the fluxgate magnetometer.

Parameters	*Value*	*Unit*	*Parameters*	*Value*	*Unit*
The length of the boom 1,2, and 3 (l)	1	m	Density	1650	kg/m^3
The radius of the boom 1 (R_1, r_1)	(20, 17.5)	mm	Elastic modulus	288	GPa
The radius of the boom 2 (R_2, r_2)	(25, 22.5)	mm	Poisson's ratio	0.266	
The radius of the boom 3 (R_3, r_3)	(30, 27.5)	mm	Horizontal stiffness coefficients (k^h_{lin},k^h_{nl})	(6×10^6, 8×10^8)	(N/m, N/m^3)
Vertical stiffness coefficients (k^v_{lin},k^v_{nl})	(8×10^5, 8×10^8)	(N/m, N/m^3)	Rotational stiffness coefficients (k^r_{lin},k^r_{nl})	(9×10^4, 9×10^7)	(N·m/rad, N·m/rad^3)

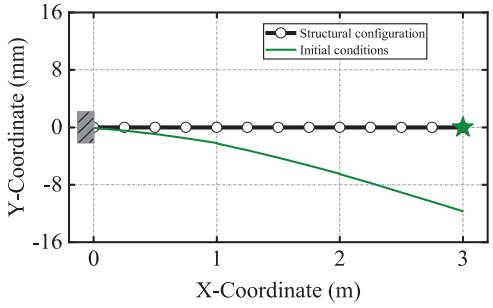

Fig. 5. Initial displacement conditions for the periodic vibration (T=0.0747s) of the magnetometer boom: black curve means the structural configuration, green curve means the initial conditions, the white dots are nodes of the FE model, and the green star is the selected node 16.

the basic beam-spring finite element model can also be applied to a similar and complex space truss structure [52]. To consider the nonlinearity in the hinges, the cubic springs are generally used for the equivalent modeling in the beam-spring FE model [9,53]. The stiffness coefficients of the hinge shown in Table 5 are pre-given for the numerical analysis. The crucial issues on model updating of the local nonlinear hinges are then discussed by the following descriptions.

3.2.1. Modelling of boom with nonlinear hinges

The beam-spring FE model consists of 16 nodes, 12 Euler-Bernoulli beam elements, and 3 nonlinear spring elements. The total DOF of the FE model is 45. The relationship between displacement and nonlinear restoring force satisfies the following equation,

$$f = f_{lin} + f_{nl} = kx + k_{nl}x^3 \tag{28}$$

in which the k_{lin} and k_{nl} denote the linear and cubic nonlinear stiffness coefficients, respectively. The linear one can be directly added into the structural stiffness matrix, and the nonlinear one is introduced as follows.

The general configuration of the nonlinear spring elements which are applied to connect several separate components is shown in Fig. 4(c). Two types, internal type (element α) and grounded type (element β), of the nonlinear spring element, is considered in this paper. For every element, three physical DOF, i.e. , the horizontal, vertical, and rotational DOF, are considered at every node like node i and j. The nonlinear restoring force vector $\mathbf{f}_{nl}(\mathbf{x}(\theta,t),\theta)$ is written as:

$$\mathbf{f}_{nl}(\mathbf{x}(\theta,t),\theta) = \sum \mathbf{f}^{\alpha}_{nl} \tag{29}$$

where $\mathbf{f}^{\alpha}_{nl}$ is the nonlinear restoring force of the α^{th} nonlinear element, which is obtained based on the relative or absolute displacements [16]. In this example, the nonlinear restoring force of the beam-like FE model

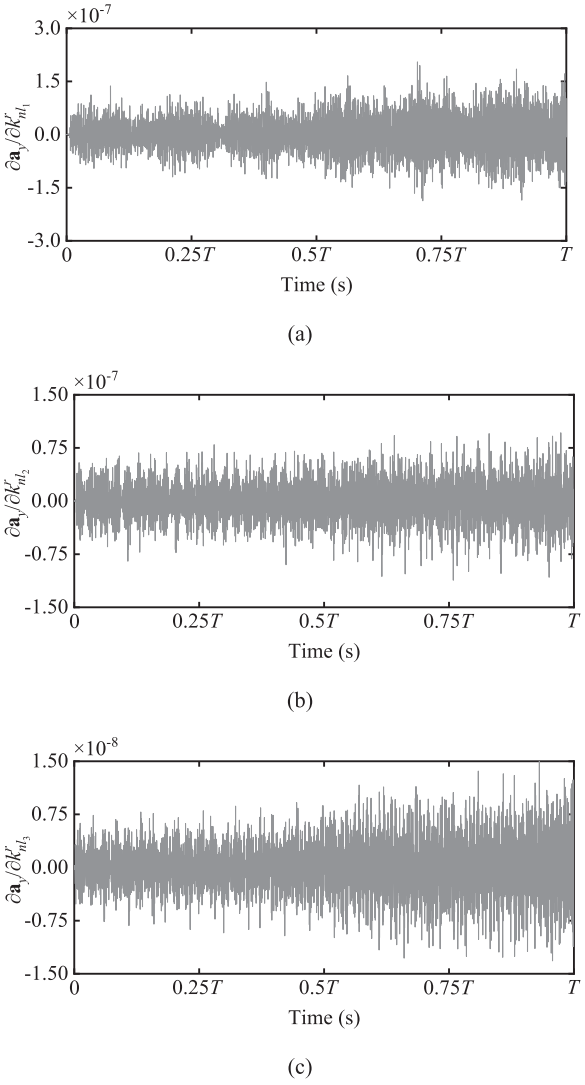

Fig. 6. Dynamic sensitivity of y-acceleration at point 16 with respect to updating parameters: (a)$\partial\mathbf{a}_y/\partial k^r_{nl_1}$, (b)$\partial\mathbf{a}_y/\partial k^r_{nl_2}$, (c)$\partial\mathbf{a}_y/\partial k^r_{nl_3}$.

is given by,

$$\mathbf{f}_{nl} = \begin{Bmatrix} k^h_{nl}x^3_1 \\ k^v_{nl}y^3_1 \\ k^r_{nl}\theta^3_1 \\ \vdots \\ k^h_{nl}(x_{13}-x_{16})^3 \\ k^v_{nl}(y_{14}-y_{17})^3 \\ k^r_{nl}(\theta_{15}-\theta_{18})^3 \\ k^h_{nl}(x_{16}-x_{13})^3 \\ k^v_{nl}(y_{17}-y_{14})^3 \\ k^r_{nl}(\theta_{18}-\theta_{15})^3 \\ \vdots \end{Bmatrix} \tag{30}$$

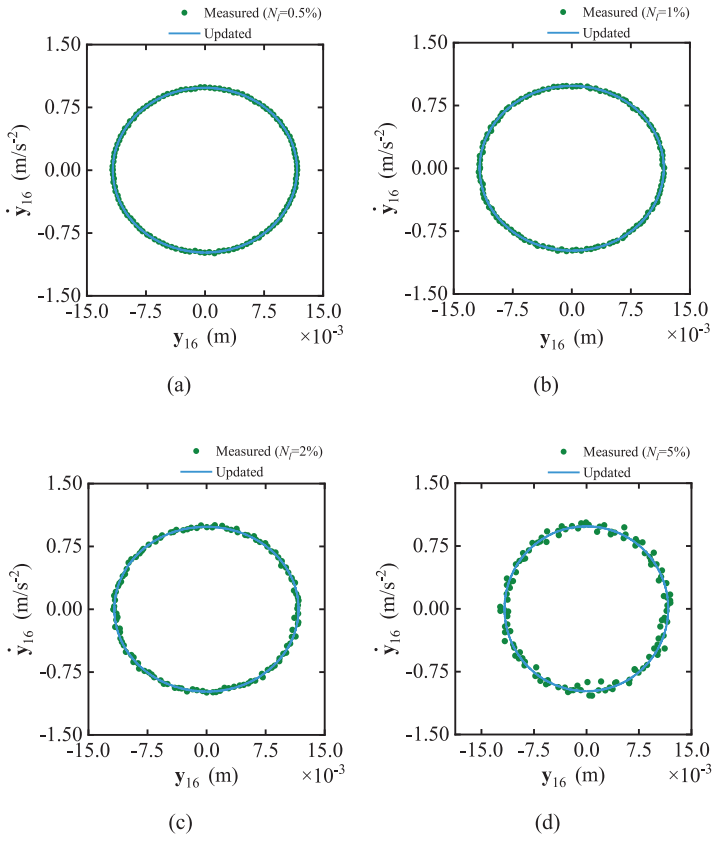

Fig. 7. Measured and updated phase diagrams for different noise levels: (a) N_l=0.5%; (b) N_l=1%; (c) N_l=2%; (d) N_l=5%.

Table 6
The relative ratio of the updated rotational stiffness coefficients of the nonlinear hinges for different initial parameters.

Initial parameters (N•m/rad^3)	r_1	r_2	r_3
Set 1: (5.85,4.5,13.95) ×10^7	1.000	1.000	0.996
Set 2: (10.8,11.3,6.59) ×10^7	1.000	1.000	0.997
Set 3: (4,16,5) ×10^7	1.000	1.000	1.003
Set 4: (2,16,4) ×10^7	0.998	1.005	1.111

Table 7
The relative ratio of the updated rotational stiffness coefficients of the nonlinear hinges for different noise levels.

Noise level (%)	r_1	r_2	r_3
N_l=0	1.000	1.000	0.996
N_l=0.5	0.995	1.013	1.015
N_l=1	1.008	1.007	0.985
N_l=2	0.993	0.962	1.098
N_l=5	0.942	1.005	0.814

The rotational stiffness coefficients of the cubic terms for the three hinges are selected as the updating parameters in this case. The initial velocities are zero, and the initial displacements are shown in Fig. 5. The time interval is [0, T], and the corresponding time step is $\Delta t=T/N_T$, where T is the minimal period of the NNM motion and determined from the shooting and pseudo-arclength continuation algorithm [54], N_T is the number of the time interval. A small time-step is used for ensuring the accuracy of the integration procedure [27], e.g., N_T=3000. To evaluate how the initial parameters will affect the updated results, different initial parameters ($k^r_{nl_1}$,$k^r_{nl_2}$,$k^r_{nl_3}$) for three nonlinear hinges are used in the nonlinear FE model updating.

The simulated dynamic responses and corresponding sensitivities are solved by the proposed method in Section 2.1. The y-acceleration without noise at point 16 is selected as the targeted outputs, and the selection control variable is set to γ=2/3 for the updating process. The sensitivities of acceleration at point 16 with respect to updating parameters are shown in Fig. 6. The convergency criterion is the same as shown in Section 3.1. By adopting the proposed nonlinear FE model updating method, the relative ratios for the updated parameters considering different initial parameters, i.e., $r=\theta^{\text{updated}}/\theta^{\text{exact}}$, are presented in Table 6. The relative errors for set 4 are 0.2%, 0.5%, and 11.1% for these three parameters ($k^r_{nl_1}$,$k^r_{nl_2}$,$k^r_{nl_3}$), respectively. The relative error is less than 0.5% for other sets. It is reasonable since the dynamic sensitivity to the local parameters is small than that to global parameters (e.g., density and modulus), and the dynamic sensitivity to $k^r_{nl_3}$ shown in Fig. 6(c) is small than that to other updating parameters. The results indicate that the local hinge parameters can be well updated using the proposed method for different initial parameters.

3.2.2. *Effect of the measurement noise*

The initial parameters of Set 1 in Table 6 are used in this subcase. The measurement random noises with level N_l=0.5%, 1%, 2%, and 5% are considered. The y-acceleration with different noise levels at point 16 is selected as the targeted outputs, and the selection control variable is set to γ=2/3 for the updating process. The other parameters for the proposed nonlinear FE model updating process are the same as the above.

The updated and measured phase diagrams for the four sets are shown in Fig. 7. The relative ratios of the updated hinge parameters are represented in Table 7. As with the same performance in Section 3.1, the local parameters can be successfully updated under low noise level, herein, the maximum relative error equals to 1.5% (r_3=0.985) for noise N_l=1%. Under high noise levels N_l=2% and N_l=5%, the relative ratios are r_3=1.098(e_3=9.8%) and r_3=0.814(e_3=18.6%), respectively. It is explainable since the low sensitivity of the dynamic responses with re-

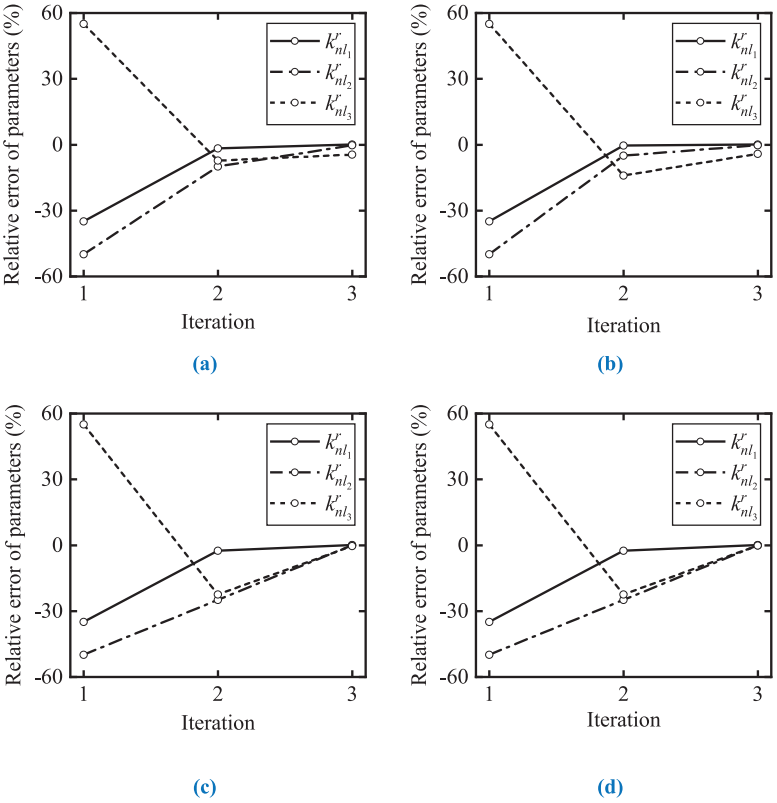

Fig. 8. History of the relative error of parameters in the updating procedure for different selection control variables: (a) γ=1/6 (b) γ=1/3; (c) γ=2/3; (d) γ=1.

Table 8
The relative ratio of the updated rotational stiffness coefficients of the nonlinear hinges for different selection control variables.

γ	r_1	r_2	r_3
1/6	1.001	0.997	0.954
1/3	1.001	0.998	0.958
2/3	1.000	1.000	0.996
1	1.000	1.000	0.999

spect to the rotational stiffness coefficients of the local nonlinear hinges, which is shown in Fig. 6. The results indicate that the proposed approach works well under different measurement noise levels.

3.2.3. Effect of the selection of the targeted responses

The issue of the selection of the targeted responses used in nonlinear FE model updating is investigated in this subcase. The initial parameters of Set 1 in Table 6 are used in this subcase. The noise level is set to zero, and the selection control variable is γ=1/6, 1/3, 2/3, and 1. The time interval is also [0, T], and other parameters for the nonlinear FE model updating process are the same as the Section 3.2.1.

As shown in Fig. 1, the procedure stops until any of the response errors or parameter estimation errors satisfy the convergence criteria, which are given in Section 2.2. After four steps of iteration, the stiffness coefficients converge for all sets of control variables. The history of the relative errors of the updating parameters is shown in Fig. 8. Updated parameters compared with the exact values are presented in Table 8. In the magnetometer boom case, the relative errors of initial responses for different selection control variables calculated using Eq (21) are 0.89%, 0.97%, 1.16%, and 1.41%, respectively. These initial response errors are smaller than that of the first case, and all the parameters can be accurately updated using the proposed method. The maximum error of updated parameters decreases with the increases of the control variables,

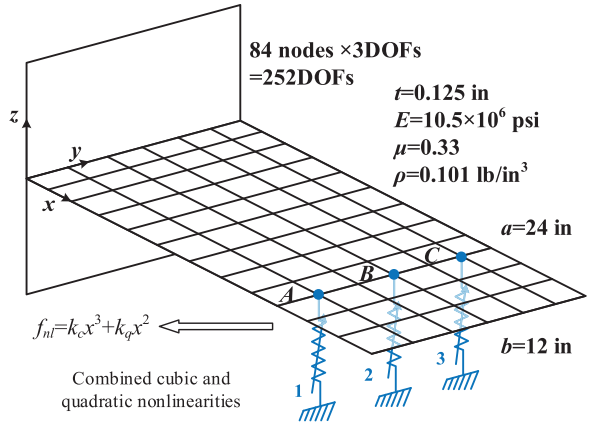

Fig. 9. A cantilever plate with multiple nonlinear supports.

and $e_{\max}$ is 4.6% in the set of γ=1/6 for $k^r_{nl_3}$. With a small relative error of initial responses, the updating results of parameters are becoming stable when the control variable γ is larger than 2/3. Results show that the accurate nonlinear FE model can be determined based on the proposed method after a small amount number of iterations.

3.3. Cantilever plate with multiple nonlinear supports

In order to show the applicability of the present method, a cantilever plate with multiple nonlinear supports is shown in Fig. 9. The linear component of the structure was proposed by Kim [55], and the elastic supports with combined cubic and quadratic nonlinear stiffness effect located at points *A*, *B*, and *C* were considered in this case. The nonlinear force for each support is calculated using equation: $f_{nl}=k_c x^3+k_q x^2$, and six parameters are selected to be updated. The material and geometric

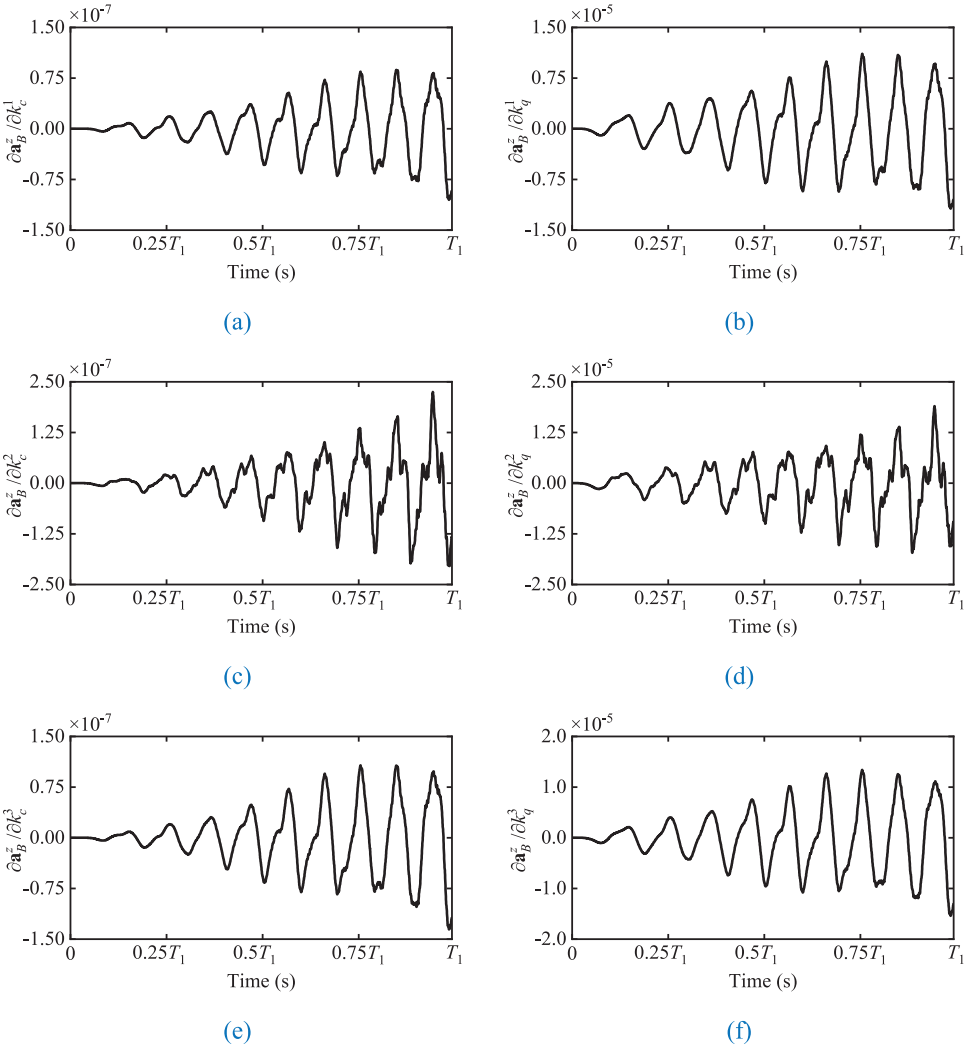

Fig. 10. Dynamic sensitivity of the z-acceleration of point B with respect to updating cubic and quadratic parameters: (a)$\partial \mathbf{a}_B^z/\partial k_c^1$, (b)$\partial \mathbf{a}_B^z/\partial k_q^1$, (c) $\partial \mathbf{a}_B^z/\partial k_c^2$, (d) $\partial \mathbf{a}_B^z/\partial k_q^2$, (e) $\partial \mathbf{a}_B^z/\partial k_c^3$, (f) $\partial \mathbf{a}_B^z/\partial k_q^3$.

Table 9
Exact and initial values of the cubic and quadratic parameters.

Parameters	*Exact*	*Initial*
k_c^1 (lbf/in^3)	1×10^5	1.2×10^5
k_q^1 (lbf/in^2)	5×10^4	5.4×10^4
k_c^2 (lbf/in^3)	1×10^5	0.7×10^5
k_q^2 (lbf/in^2)	5×10^4	4.7×10^4
k_c^3 (lbf/in^3)	1×10^5	0.8×10^5
k_q^3 (lbf/in^2)	5×10^4	5.2×10^4

Table 10
The relative ratio and errors for the updated parameters with different measurement noise levels.

Parameters	N_l=0		N_l=2%	
	r	*e* (%)	*r*	*e* (%)
k_c^1	1.010	1.0	0.989	1.1
k_q^1	1.000	0	1.000	0
k_c^2	0.987	1.3	0.945	5.5
k_q^2	1.000	0	1.001	0.1
k_c^3	1.010	1.0	0.982	1.8
k_q^3	1.000	0	1.000	0

properties are given in Fig. 9, and the structure is modeled by 12×6 plate FE elements. Three displacement components, i.e., a deflection (w_z) and two in-plane rotations (θ_x and θ_y), are considered in the plate FE element, and the total DOFs of the structure is 252. The pre-given exact and initial values of the updating parameters are listed in Table 9.

The forced vibration under external force, $f_B^z(t) = 10\sin(\omega_1 t)$, is considered in this case, and the initial displacements and velocities are set to zero. ω_1 is the first natural frequency of the linear components of the structure, ω_1=0.37Hz. The time interval is [0, T_1], and the corresponding time step is $\Delta t = T_1/N_T$, where T_1 and N_T are $T_1 = 1/\omega_1$, and N_T=3000, respectively. The z-direction accelerations with the different noise levels, N_l=0, and N_l=2%, at points *A*, *B*, and *C*, are selected to update these six parameters. Using the direct sensitivity analysis approach, the nonlinear dynamic responses and corresponding sensitivities can be calculated synchronously. The dynamic sensitivity of the acceleration at point B with respect to six updating parameters are shown in Fig. 10. The magnitudes of dynamic sensitivity of the acceleration with respect to quadratic parameters are larger than that of the acceleration with respect to cubic parameters. The accuracy of the updated cubic parameters has been affected by this situation. The initial error of the selected accelerations with full data points is 10.83%, and these updating parameters are also of the local nonlinear parameters. The selection control variable, therefore, is set to γ=1 to ensure the accuracy of the nonlinear FE model updating.

Table 10 illustrate the relative ratio and error of the updated parameters compared to the exact values. These errors for noise-free and 2% simulated noise cases are less than 6%, indicating that a good agreement

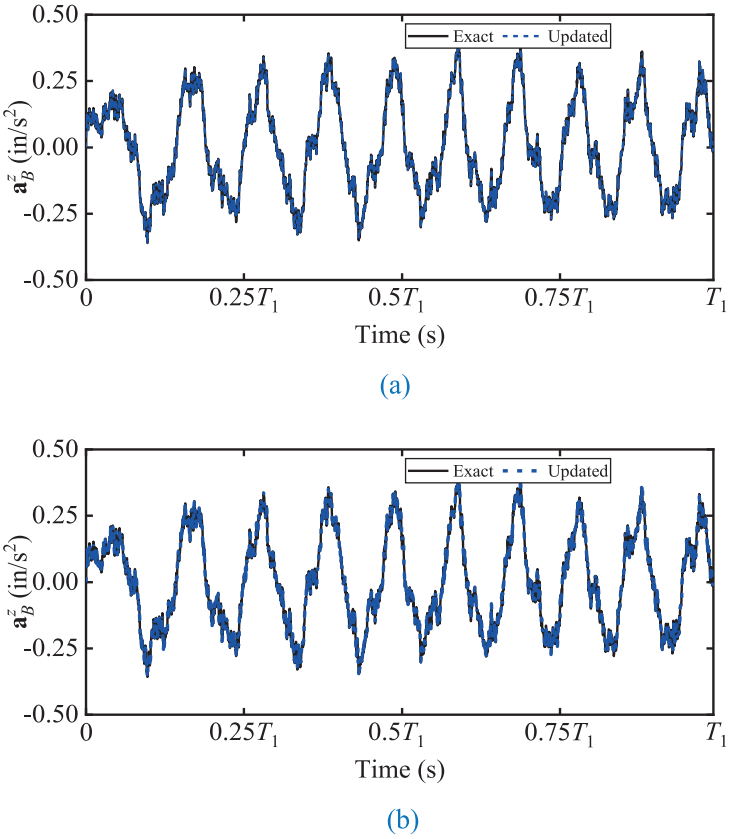

Fig. 11. Updated acceleration $\mathbf{a}^z_B$ compared to the exact responses with different measurement noise levels: (a) N_l=0, (b) N_l=2%.

between the updated and exact parameters can be obtained using the proposed method. The maximum error is 5.5% for k_c^2 (N_l=2%) among all the parameter updating results, illustrating that the inaccuracy of updated nonlinear parameters is increased with an increase in the noise level, and the insensitive parameters are more affected by the measurement noise. The acceleration with different noise levels calculated from the updated nonlinear FE model and the exact responses are compared and shown in Fig. 11(a) and (b), respectively. Results show that the proposed dynamic sensitivity-based nonlinear FE model updating method is applicable for updating a complex structure modelled using commercial FE software, even under a low noise level effect.

4. Conclusion

A dynamic sensitivity-based model updating approach for nonlinear structures is proposed in this paper. The updating method is carried out using the time-domain responses. The effects of the nonlinear structural parameters on the time-domain responses are evaluated based upon the dynamic sensitivity analysis, which is directly and simultaneously calculated from the differentiation of the first-order or second-order equations of motion.

The accuracy and advantage of the proposed method are verified using different numerical models. The effect of the noise in the time-domain responses and the selection scheme of the targeted responses points are investigated. Based on the simulation results, the following conclusions are obtained. (1) The time-domain responses can be adopted for nonlinear FE model updating even the observations are with noise. (2) The scheme for selecting the response points guarantees the accuracy of the updated nonlinear FE model when considering different relative errors of the initial responses. (3) A small amount number of iterations of the updating process are the advantage of the proposed method.

The proposed nonlinear FE model updating approach is applicable to the structure whose dynamic sensitivity is calculated by direct differentiation. The proposed approach, however, does not account for the non-smooth nonlinearity and the actual measurement noise. Experimental verification on the proposed approach for a complex structure considering gap and contact is worthy of further study.

Author statement

The authors are appreciative of the constructive comments and suggestions provided by the reviewers.

Declaration of Competing Interest

The authors declare that they have no known competing financial interests or personal relationships that could have appeared to influence the work reported in this paper.

CRediT authorship contribution statement

Zhifu Cao: Conceptualization, Methodology, Software, Validation, Formal analysis, Investigation, Data curation, Writing - original draft, Writing - review & editing, Visualization. **Qingguo Fei:** Resources, Writing - review & editing, Project administration, Supervision, Funding acquisition. **Dong Jiang:** Investigation, Validation, Writing - review & editing. **Dahai Zhang:** Writing - review & editing. **Hui Jin:** Writing - review & editing. **Rui Zhu:** Writing - review & editing.

Acknowledgments

The authors would like to thank the support of the National Natural Science Foundation of China (No. 11602112, No. 11572086), and the Natural Science Foundation of Jiangsu Province (No.BK20170022, No.BK20190324), and the National Key Research and Development Program of China (2017YFC0805103), and the Fundamental Research Funds for the Central Universities.

Table A1
Pseudo-code for nonlinear dynamic response and sensitivity analysis.

Pseudo-code 1 Nonlinear dynamic response and sensitivity
Input: Initial conditions: $\mathbf{x}_0$, $\dot{\mathbf{x}}_0$, $\mathbf{S}$, $\dot{\mathbf{S}}_0$, $\ddot{\mathbf{S}}_0$; Structural matrices: **M, C, K**; External excitation: $\mathbf{f}(t)$; Nonlinear elements parameters: θ; Newmark scheme parameter: t_f, N_T, β, α
Output: Calculated nonlinear responses: $\mathbf{x},\dot{\mathbf{x}},\ddot{\mathbf{x}}$; Dynamic sensitivities: $\mathbf{S},\dot{\mathbf{S}},\ddot{\mathbf{S}}$
Begin
$\mathbf{f}_{nl0}=\mathbf{f}_{nl}(\mathbf{x}_0,\dot{\mathbf{x}}_0,\boldsymbol{\theta})$ // Initial nonlinear force
$\ddot{\mathbf{x}}_0=\mathbf{M}^{-1}(\mathbf{f}_0-\mathbf{C}\dot{\mathbf{x}}_0-\mathbf{K}\mathbf{x}_0-\mathbf{f}_{nl0})$ // Initial acceleration
$\Delta t=t_f/N_T$ // Time-step
for *time*=1 to t_f // Final time
$t_{i+1}:=t_i+\Delta t$ // Computation time
$\dot{\mathbf{x}}_{i+1}:=\dot{\mathbf{x}}_i+(1-\alpha)\,\Delta t\ddot{\mathbf{x}}_i$; $\mathbf{x}_{i+1}:=\mathbf{x}_i+\Delta t\dot{\mathbf{x}}_i+(1/2-\beta)\Delta t^2\ddot{\mathbf{x}}_i$; $\ddot{\mathbf{x}}_{i+1}:=\mathbf{0}$; // Prediction
$\mathbf{f}_{nli+1}:=\mathbf{f}_{nl}(\mathbf{x}_{i+1},\dot{\mathbf{x}}_{i+1},\boldsymbol{\theta})$; $\mathbf{K}_T$ // Predicted nonlinear force and tangent stiffness matrix
$e^R:=||\mathbf{M}\ddot{\mathbf{x}}_{i+1}+\mathbf{C}\dot{\mathbf{x}}_{i+1}+\mathbf{K}\mathbf{x}_{i+1}+\mathbf{f}_{nli+1}-\mathbf{f}_{i+1}||/||\mathbf{M}\ddot{\mathbf{x}}_{i+1}+\mathbf{C}\dot{\mathbf{x}}_{i+1}+\mathbf{K}\mathbf{x}_{i+1}+\mathbf{f}_{nli+1}||$ // Relative error of prediction responses
if $e^R>\varepsilon$ ***then***
$\mathbf{K}_e^R:=\frac{1}{\alpha\Delta t^2}\mathbf{M}+\frac{\beta}{\alpha\Delta t}\mathbf{C}+\mathbf{K}+\mathbf{K}_T$ // Equivalent stiffness matrix for nonlinear dynamic response calculation
$\mathbf{F}_e^R:=\mathbf{M}\ddot{\mathbf{x}}_{i+1}+\mathbf{C}\dot{\mathbf{x}}_{i+1}+\mathbf{K}\mathbf{x}_{i+1}+\mathbf{f}_{nl_{i+1}}-\mathbf{f}_{i+1}$ // Equivalent residual vector for nonlinear dynamic response calculation
$\Delta\mathbf{x}:=-(\mathbf{K}_e^R)^{-1}\mathbf{F}_e^R$ // Increment displacement calculation
$\mathbf{x}_{i+1}:=\mathbf{x}_{i+1}+\Delta\mathbf{x}$; $\dot{\mathbf{x}}_{i+1}:=\dot{\mathbf{x}}_{i+1}+\alpha/(\beta\Delta t)\Delta\mathbf{x}$; $\ddot{\mathbf{x}}_{i+1}:=\ddot{\mathbf{x}}_{i+1}+1/(\beta\Delta t^2)\Delta\mathbf{x}$; // Correction
$\mathbf{f}_{nli+1}:=\mathbf{f}_{nl}(\mathbf{x}_{i+1},\dot{\mathbf{x}}_{i+1},\boldsymbol{\theta})$; $\mathbf{K}_T$ // Updated nonlinear force and tangent stiffness matrix
$e^R:=||\mathbf{M}\ddot{\mathbf{x}}_{i+1}+\mathbf{C}\dot{\mathbf{x}}_{i+1}+\mathbf{K}\mathbf{x}_{i+1}+\mathbf{f}_{nli+1}-\mathbf{f}_{i+1}||/||\mathbf{M}\ddot{\mathbf{x}}_{i+1}+\mathbf{C}\dot{\mathbf{x}}_{i+1}+\mathbf{K}\mathbf{x}_{i+1}+\mathbf{f}_{nli+1}||$ // Relative error of updated responses
end if
$\mathbf{J}_{\mathbf{x},i+1}$, $\mathbf{J}_{\dot{\mathbf{x}},i+1}$ // Jacobian matrices of nonlinear force with respect to displacement and velocity
$\frac{\partial\mathbf{f}_{nl}(\mathbf{x}_{i+1},\dot{\mathbf{x}}_{i+1},\boldsymbol{\theta})}{\partial\boldsymbol{\theta}}$ // Derivative of nonlinear force with respect to updating parameters
$\mathbf{K}_e^s:=\frac{1}{\beta(\Delta t)^2}\mathbf{M}+\frac{\alpha}{\beta(\Delta t)}(\mathbf{C}+\mathbf{J}_{\dot{\mathbf{x}},n+1})+(\mathbf{K}+\mathbf{J}_{\mathbf{x},n+1})$ // Equivalent stiffness matrix for dynamic sensitivity calculation
$\mathbf{F}_e^s:=\mathbf{M}(-\frac{1}{\beta\Delta t^2}\mathbf{S}_i-\frac{1}{\beta\Delta t}\dot{\mathbf{S}}_i+(1-\frac{1}{2\beta})\ddot{\mathbf{S}}_i)$
$+(\mathbf{C}+\mathbf{J}_{\dot{\mathbf{x}}_{i+1}})(-\frac{\alpha}{\beta\Delta t}\mathbf{S}_i+(1-\frac{\alpha}{\beta})\dot{\mathbf{S}}_i+\Delta t(1-\frac{\alpha}{2\beta})\ddot{\mathbf{S}}_i)$ // Equivalent residual vector for dynamic sensitivity calculation
$+\frac{\partial\mathbf{f}_{nl}(\mathbf{x}_{i+1},\dot{\mathbf{x}}_{i+1})}{\partial\boldsymbol{\theta}}$
$\mathbf{S}_{i+1}:=-(\mathbf{K}_e^s)^{-1}\mathbf{F}_e^s$// Displacement sensitivity
$\dot{\mathbf{S}}_{i+1}:=\frac{\alpha}{\beta\Delta t}(\mathbf{S}_{i+1}-\mathbf{S}_i)+(1-\frac{\alpha}{\beta})\dot{\mathbf{S}}_i+\Delta t(1-\frac{\alpha}{2\beta})\ddot{\mathbf{S}}_i$ // Velocity sensitivity
$\ddot{\mathbf{S}}_{i+1}:=\frac{1}{\beta\Delta t^2}(\mathbf{S}_{i+1}-\mathbf{S}_i)-\frac{1}{\beta\Delta t}\dot{\mathbf{S}}_i-(\frac{1}{2\beta}-1)\ddot{\mathbf{S}}_i$ // Acceleration sensitivity
end for
end

Table A2
Pseudo-code for nonlinear FE model updating based on direct sensitivity analysis.

Pseudo-code 2 Direct sensitivity-based nonlinear FE model updating
Input: Measured responses: $\mathbf{R}^m$; Initial parameters: $\boldsymbol{\theta}_0$; Selection control variable: γ; Maximum number of iterations: N; Nonlinear dynamic responses and sensitivity analysis parameters: $\mathbf{x}_0$, $\dot{\mathbf{x}}_0$, t_f, N_T, **K, M, C,** $\mathbf{f}(t)$, $\mathbf{f}_{nl}$
Output: Updated parameters: $\boldsymbol{\theta}^{updated}$; Updated responses: $\mathbf{R}^{updated}$
Begin
$r_p:=1$ to γN_T// Selected responses points
for *iteration*=1 to N // Maximum number of iterations
$n+1:=n$
$\mathbf{R}_n$, $\mathbf{S}_n$ // Calculated nonlinear dynamic responses and sensitivities using $\mathbf{x}_0$, $\dot{\mathbf{x}}_0$, t_f, N_T, **K, M, C,** $\mathbf{f}(t)$, $\mathbf{f}_{nl}$ in **Pseudo-code 1**
$\mathbf{r}_n:=\mathbf{R}^m-\mathbf{R}_n$ // Response residual
$\Delta\boldsymbol{\theta}\leftarrow\min J_{non}(\boldsymbol{\theta})=\frac{1}{2}\sum_{q=1}^{N_q}\sum_{k=1}^{N_t}\|W_{\boldsymbol{\alpha}(t,\boldsymbol{\theta})}(R_q^m(t_k)-R_q(t_k,\boldsymbol{\theta}))\|_2^2$ // Updating parameters estimation using the optimization method in MATLAB
$\boldsymbol{\theta}_{n+1}:=\boldsymbol{\theta}_n+\Delta\boldsymbol{\theta}$ // Updated parameters
$e_r:=\frac{\|\mathbf{R}^m-\mathbf{R}_n\|_2}{\|\mathbf{R}^m\|_2}\times100\%$ // Responses error
$e_\theta:=\frac{\|\Delta\boldsymbol{\theta}\|_2}{\|\boldsymbol{\theta}_n\|_2}\times100\%$ // Parameter estimation error
if e_r or e_θ < *tolerance* ***then***
Return
else
Continue
end if
end for
end

Appendix A. Pseudo-code for direct sensitivity-based nonlinear FE model updating

Tables A1 and A2.

Appendix B. Dynamic sensitivity analysis of Duffing-Van der Pol oscillator

The first-order form of the Duffing-Van der Pol oscillator is given in Eq. (26). The new unknowns are given as follows

$$\boldsymbol{\zeta}=\begin{Bmatrix}x\\ y\\ \dfrac{\partial x}{\partial\boldsymbol{\theta}}\\ \dfrac{\partial y}{\partial\boldsymbol{\theta}}\end{Bmatrix} \tag{B1}$$

where

$$\begin{cases} \dfrac{\partial x}{\partial \theta} = \left[\dfrac{\partial x}{\partial \mu} \quad \dfrac{\partial x}{\partial \alpha} \quad \dfrac{\partial x}{\partial \beta}\right]^T = \left[s_{11} \quad s_{12} \quad s_{13}\right]^T \\ \dfrac{\partial y}{\partial \theta} = \left[\dfrac{\partial y}{\partial \mu} \quad \dfrac{\partial y}{\partial \alpha} \quad \dfrac{\partial y}{\partial \beta}\right]^T = \left[s_{21} \quad s_{22} \quad s_{23}\right]^T \end{cases} \tag{B2}$$

in which the updating parameters herein are $\theta=[\mu,\ \alpha,\ \beta]^T$. Finally, the first-order equations of motion and sensitivity have the form

$$\dot{\boldsymbol{\zeta}} = \begin{Bmatrix} \dot{x} \\ \dot{y} \\ \dot{s}_{11} \\ \dot{s}_{12} \\ \dot{s}_{13} \\ \dot{s}_{21} \\ \dot{s}_{22} \\ \dot{s}_{23} \end{Bmatrix} = \begin{Bmatrix} y \\ \mu\left(1-x^2\right)y - \alpha x - \beta x^3 + f\cos(\omega t) \\ s_{21} \\ s_{22} \\ s_{23} \\ \left(1-x^2\right)y - 2\mu x y s_{11} + \mu\left(1-x^2\right)s_{21} - \alpha s_{11} - 3\beta x^2 s_{11} \\ -2\mu x y s_{12} + \mu\left(1-x^2\right)s_{22} - x - \alpha s_{12} - 3\beta x^2 s_{12} \\ -2\mu x y s_{13} + \mu\left(1-x^2\right)s_{23} - \alpha s_{13} - x^3 - 3\beta x^2 s_{13} \end{Bmatrix} \tag{B3}$$

The initial conditions are given in advance, so the initial sensitivities of displacement and velocity are zero. The dynamic and sensitivity equations (B3) can be solved using Runge-Kutta method, which is integrated into the 'ode45' function of MATLAB.

References

[1] Bui TQ, Vo DQ, Zhang C, Nguyen DD. A consecutive-interpolation quadrilateral element (CQ4): formulation and applications. Finite Elem Anal Des 2014;84:14–31.
[2] Nguyen MN, Bui TQ, Truong TT, Trinh NA, Singh IV, Yu T, Doan DH. Enhanced nodal gradient 3D consecutive-interpolation tetrahedral element (CTH4) for heat transfer analysis. Int J Heat Mass Transf. 2016;103:14–27.
[3] Nguyen MN, Bui TQ, Truong TT, Tanaka S, Hirose S. Numerical analysis of 3-D solids and composite structures by an enhanced 8-node hexahedral element. Finite Elem Anal Des 2017;131:1–16.
[4] Mottershead JE, Link M, Friswell MI. The sensitivity method in finite element model updating: a tutorial. Mech Syst Signal Pr 2011;25(7):2275–96.
[5] Jang J, Smyth AW. Model updating of a full-scale FE model with nonlinear constraint equations and sensitivity-based cluster analysis for updating parameters. Mech Syst Signal Pr 2017;83:337–55.
[6] Zhao W, Gupta A, Miglani J, Regan CD, Kapania RK, Seiler PJ. Finite element model updating of composite flying-wing aircraft using global/local optimization. In: AIAA Scitech 2019 Forum; 2019. p. 1–36.
[7] Jiang D, Wu SQ, Shi QF, Fei QG. Contact interface parameter identification of bolted joint structure with uncertainty using thin layer element method. Eng Mech 2015;32(4):220–7.
[8] Hernández S, Menga E, Naveira P, Freire D, López C, Cid Montoya M, Moledo S, Baldomir A. Dynamic analysis of assembled aircraft structures considering interfaces with nonlinear behavior. Aerosp Sci Technol 2018;77:265–72.
[9] Cao ZF, Fei QG, Jiang D, Wu SQ, Liu JZ. Nonlinear normal modal analysis of flexible structures with nonlinear hinge. J Vib Eng 2018;31(4):573–81.
[10] Jiang D, Zhang DH, Fei QG, Wu SQ. An approach on identification of equivalent properties of honeycomb core using experimental modal data. Finite Elem Anal Des 2014;90:84–92.
[11] Jiang D, Li YB, Fei QG, Wu SQ. Prediction of uncertain elastic parameters of a braided composite. Compos Struct 2015;126:123–31.
[12] Cao ZF, Fei QG, Jiang D, Wu SQ, Fan ZR. Model updating of a stitched sandwich panel based on multistage parameter selection. Math Probl Eng 2019:1–15.
[13] Ewins DJ, Weekes B, Carri AD. Modal testing for model validation of structures with discrete nonlinearities, philosophical transactions of the royal society A-mathematical. Phys, Eng Sci 2015;373:20140410.
[14] Carri AD, Weekes B, Maio DD, Ewins DJ. Extending modal testing technology for model validation of engineering structures with sparse nonlinearities: a first case study. Mech Syst Signal Pr 2017;84:97–115.
[15] Cooper SB, DiMaio D, Ewins DJ. Integration of system identification and finite element modelling of nonlinear vibrating structures. Mech Syst Signal Pr 2018;102:401–30.
[16] Wang X, Hill TL, Neild SA, Shaw AD, Haddad KH, Friswell MI. Model updating strategy for structures with localised nonlinearities using frequency response measurements. Mech Syst Signal Pr 2018;100:940–61.
[17] Asgarieh E, Moaveni B, Stavridis A. Nonlinear finite element model updating of an infilled frame based on identified time-varying modal parameters during an earthquake. J Sound Vib 2014;333:6057–73.
[18] Wang ZC, Xin Y, Ren WX. Nonlinear structural model updating based on instantaneous frequencies and amplitudes of the decomposed dynamic responses. Eng Struct 2015;100:189–200.
[19] Wang ZC, Xin Y, Ren WX. Nonlinear structural joint model updating based on instantaneous characteristics of dynamic responses. Mech Syst Signal Pr 2016;76–77:476–96.
[20] Kurt M, Eriten M, McFarland DM, Bergman LA, Vakakis AF. Methodology for model updating of mechanical components with local nonlinearities. J Sound Vib 2015;357:331–48.
[21] Kurt M, Moore KJ, Eriten M, McFarland DM, Bergman LA, Vakakis AF. Nonlinear model updating applied to the IMAC XXXII round Robin benchmark system. Mech Syst Signal Pr 2017;88:111–22.
[22] Damme CIV, Allen MS, Hollkamp JJ. Nonlinear structural model updating based upon nonlinear normal modes. 2018 AIAA/ASCE/AHS/ASC Structures, Structural Dynamics, and Materials Conference, American Institute of Aeronautics and Astronautics Kissimmee, Florida; 2018. pp. 0185-0181-0117.
[23] Song MM, Renson L, Noël JP, Moaveni B. Bayesian model updating of nonlinear systems using nonlinear normal modes. Struct Control Health Monit 2018;25(12) 2258-2251-2220.
[24] Silva SD, Cogan S, Foltête E, Buffe F. Metrics for nonlinear model updating in structural dynamics. J Braz Soc Mech Sci 2009;31(1):27–34.
[25] Asgarieh E, Moaveni B, Barbosa AR, Chatzi E. Nonlinear model calibration of a shear wall building using time and frequency data features. Mech Syst Signal Pr 2017;85:236–51.
[26] Wu S, Sun Y, Li Y, Fei Q. Stochastic dynamic load identification on an uncertain structure with correlated system parameters. J Vibr Acoust 2019;141(4).
[27] Bui TQ, Nguyen DD, Zhang XD, Hirose S, Batra RC. Analysis of 2-dimensional transient problems for linear elastic and piezoelectric structures using the consecutive-interpolation quadrilateral element (CQ4). Eur J Mech A/Solids 2016;58:112–30.
[28] Bui TQ, Ngoc Nguyen M, Zhang C. A moving Kriging interpolation-based element-free Galerkin method for structural dynamic analysis. Comput Methods Appl M 2011;200(13-16):1354–66.
[29] Bui TQ, Khosravifard A, Zhang CZ, Hematiyan MR, Golub MV. Dynamic analysis of sandwich beams with functionally graded core using a truly meshfree radial point interpolation method. Eng Struct 2013;47:90–104.
[30] Giovanis DG, Papaioannou I, Straub D, Papadopoulos V. Bayesian updating with subset simulation using artificial neural networks. Comput Methods Appl M 2017;319:124–45.
[31] Adel F, Shokrollahi S, Jamal Omidi M, Ahmadian H. A model updating method for hybrid composite/aluminum bolted joints using modal test data. J Sound Vib 2017;396:172–85.
[32] Chisari C, Bedon C, Amadio C. Dynamic and static identification of base-isolated bridges using genetic algorithms. Eng Struct 2015;102:80–92.
[33] Fei QG, Xu YL, Ng CL, Wong KY, Chan WY, Man KL. Structural health monitoring oriented finite element model of Tsing Ma bridge tower. Int J Struct Stab Dy 2007;7(4):647–68.
[34] Cao ZF, Fei QG, Jiang D, Wu SQ. Substructure-based model updating using residual flexibility mixed-boundary method. J Mech Sci Technol 2017;31(2):759–69.
[35] Petersen ØW, Øiseth O. Sensitivity-based finite element model updating of a pontoon bridge. Eng Struct 2017;150:573–84.
[36] Zhu T, Tian W, Weng S, Ge H, Xia Y, Wang C. Sensitivity-based finite element model updating using dynamic condensation approach. Int J Struct Stab Dyn 2017:1840004.
[37] Ebrahimian H, Astroza R, Conte JP, de Callafon RA. Nonlinear finite element model updating for damage identification of civil structures using batch Bayesian estimation. Mech Syst Signal Pr 2017;84:194–222.
[38] Zhu R, Fei QG, Jiang D, Cao ZF. Dynamic sensitivity analysis based on Sherman—Morrison–Woodbury formula. AIAA J 2019;57(11):4992–5001.
[39] Trier SD, Marthinsen A, Sivertsen OI. Design sensitivities by the adjoint variable method in nonlinear structural dynamics. In: SIMS simulation conference; 1996. p. 1–8.
[40] Kim N, Choi K. Design sensitivity analysis and optimization of nonlinear transient dynamics. In: 8th AIAA/USAF/NASA/ISSMO Symposium on Multidisciplinary Analysis and Optimization; 2000. p. 1–11.
[41] Keulen FV, Haftka RT, Kim NH. Review of options for structural design sensitivity analysis. Part 1: linear systems. Comput Methods Appl M 2005;194(30):3213–43.
[42] Conte JP, Vijalapura PK, Meghella M. Consistent finite-element response sensitivity analysis. J Eng Mech 2003;129(12):1380–93.
[43] Gu Q, Wang G. Direct differentiation method for response sensitivity analysis of a bounding surface plasticity soil model. Soil Dyn Earthq Eng 2013;49:135–45.
[44] Scott MH, Azad VJ. Response sensitivity of material and geometric nonlinear force-based Timoshenko frame elements. Int J Numer Meth Eng 2017;111(5):474–92.
[45] Hedayatrasa S, Bui TQ, Zhang CZ, Lim CW. Numerical modeling of wave propagation in functionally graded materials using time-domain spectral Chebyshev elements. J Comput Phys 2014;258:381–404.
[46] Li XY, Law SS. Adaptive Tikhonov regularization for damage detection based on nonlinear model updating. Mech Syst Signal Pr 2010;24(6):1646–64.
[47] Nayfeh AH, Pai PF. Linear and nonlinear structural mechanics. New York: Wiley-Interscience; 2004.
[48] Chatterjee A. Parameter estimation of Duffing oscillator using Volterra series and multi-tone excitation. Int J Mech Sci 2010;52(12):1716–22.
[49] Kumar P, Narayanan S, Gupta S. Bifurcation analysis of a stochastically excited vibro-impact Duffing-Van der Pol oscillator with bilateral rigid barriers. Int J Mech Sci 2017;127:103–17.
[50] Marc DA, Ignacio M, Juan RC, Alberto L. Design of the magnetic diagnostics unit onboard LISA Pathfinder. Aerosp Sci Technol 2013;26(1):53–9.
[51] Collier MR, Connor HK. Magnetopause surface reconstruction from tangent vector observations. J Geophys Res-Space 2018;123:10189–99.

[52] Nie R, He BY, Hodges DH, Ma XF. Integrated form finding method for mesh reflector antennas considering the flexible truss and hinges. Aerosp Sci Technol 2019;84:926–37.
[53] Webster MS. Modeling beam-like space trusses with nonlinear joints with application to control. Cambridge: Massachusetts Institute of Technology; 1991.
[54] Peeters M, Viguie R, Serandour G, Kerschen G, Golinval JC. Nonlinear normal modes, Part II: Toward a practical computation using numerical continuation techniques. Mech Syst Signal Pr 2009;23(1):195–216.
[55] Kim JG, Park YJ, Lee GH, Kim DN. A general model reduction with primal assembly in structural dynamics. Comput Methods Appl M 2017;324:1–28.